Biophysical Journal

Supporting Material

MD Simulations and FRET Reveal an Environment-Sensitive Conformational Plasticity of Importin-β

Kangkan Halder,[1] Nicole Dölker,[2] Qui Van,[3] Ingo Gregor,[3] Achim Dickmanns,[4] Imke Baade,[5] Ralph H. Kehlenbach,[5] Ralf Ficner,[4] Jörg Enderlein,[3] Helmut Grubmüller,[2,*] and Heinz Neumann[1,*]

[1]Free Floater (Junior) Research Group "Applied Synthetic Biology", Institute for Microbiology and Genetics, Georg-August University Göttingen, Göttingen, Germany; [2]Department of Theoretical and Computational Biophysics, Max-Planck Institute for Biophysical Chemistry, Göttingen, Germany; and [3]Third Institute of Physics-Biophysics, [4]Institute for Microbiology and Genetics, Department of Molecular Structural Biology, and [5]Department of Molecular Biology, Faculty of Medicine, Georg-August University Göttingen, Göttingen, Germany

Supplementary Materials and Methods

Buffers and chemicals: The 4-Azido-L-phenylalanine (AzF, product code: 06162) was purchased from Chem-Impex Inter. Inc. The dibenzocyclooctyne conjugated fluorophore dye (DBCO-Fl-545, product code: CLK-A110-2, currently discontinued from manufacturer) was purchased from Jena Bioscience. The mouse monoclonal anti-His antibody (product code: 27-7410-01), enhanced chemiluminescence (ECL) Prime (product code: RPN2236) and the chemiluminescence Hyperfilm (product code: 28906837) were purchased from GE Healthcare, while the HRP-conjugated anti-Mouse IgG (product code: A4416) was acquired from Sigma Aldrich. The polyethylene glycol (PEG) of different chain lengths (200, 1,500, 3,000, 4,000 and 8,000) were purchased from either Applichem GmbH and/or Sigma Aldrich. The methanol used for titrations is HPLC grade and purchased from VWR Chemicals. Proteinase K (product code: 1092766) was purchased from Boehringer Mannheim GmbH. Vivaspin 500 (product code: Z629367) and Amicon Ultra-15 (product code: UFC903024) centrifugal concentrators were procured from Sigma Aldrich and MerckMillipore, respectively. The D-Tube Dialyzer Midi (product code: 71507-3) and Immobilon-P PVDF Transfer Membrane (product code: IPVH00010) were purchased from MerckMillipore. HisPur Ni-NTA Resin (product code: 88222) was purchased from Thermo Scientific. Other common chemicals and reagents for buffer preparation were purchased from Sigma-Aldrich, Carl Roth GmbH or Applichem. All products were stored, dissolved/ diluted, and used as per manufacturer's protocol.

Plasmids: The human Importin-β (National Center for Biotechnology Information Protein Accession Code : NP_002256.2) and superfolder green fluorescent protein (AGT98536.1) sequences were used to construct the *hs*Impβ-sfGFP-His_6, *hs*Impβ^{Q220TAG}-sfGFP-His_6 and *hs*Impβ^{Y255TAG}-sfGFP-His_6 in the pCDFDuet1 (MerckMillipore) plasmid backbone using the

standard cloning, PCR amplification, restriction enzyme digestion and ligation protocols. The T4 DNA Ligase and Phusion DNA Polymerase were obtained from Thermo Scientific, while the restriction enzymes were obtained from New England Biolabs and Thermo Scientific. The primers for cloning, site directed mutagenesis or sequencing were purchased from Sigma Aldrich as 'purified by desalting'. The plasmids were amplified in *Escherichia coli* DH10B strain in LB medium (10 g Tryptone, 5 g Yeast extract, and 5 g NaCl, in deionized water upto 1 L, pH 7.0) supplemented with Spectinomycin (50 µg/mL final) and purified by peqGOLD Plasmid Miniprep Kit (PeqLab Biotechnologie GmbH). The plasmid integrity was verified by restriction enzyme digestion and DNA sequencing. The complete plasmid sequences of the *hs*Impβ constructs are given below.

Protein Expression and Purification:

***hs*Impβ-sfGFP**: *Escherichia coli* BL21(DE3) (Merck) chemical competent cells were heat-shock transformed with plasmid pCDFDuet1_*hs*Impβ-sfGFP-His_6 and grown overnight in 100 mL of 2YT media (10 g Tryptone, 16 g Yeast extract, and 5 g NaCl, in deionized water upto 1 L, pH 7.0) with Spectinomycin (50 µg/mL) with shaking at 220 rpm at 37°C. Next morning, 1 L 2YT media with Spectinomycin (50 µg/mL) was inoculated at OD_{600} ~0.1 and grown till OD_{600} reached 0.2 – 0.3, when protein expression was induced by adding isopropyl β-D-1-thiogalactopyranoside (IPTG, 500 µM, final) and let grow for another 5 h. The cells were harvested by centrifugation at 4,800 rotations per minute (rpm), snap frozen in liquid nitrogen and stored at -80°C.

The cell pellet was resuspended in ice-cold buffer A (50 mM Tris-Cl, pH 8.0, 200 mM NaCl, 25 mM Imidazole, 1 mM phenylmethanesulfonyl-fluoride and 500 µL of ALP protease inhibitor cocktail) and disrupted by pneumatic cell disintegration using a Microfluidizer 110S (Microfluidics, USA). The cell lysate was cleared by centrifugation at 20,000 rpm, 20 min,

4°C, syringe filtered through 0.2 µm and loaded on a 5 mL Ni^{2+} sepharose HisTrap FF column (GE lifesciences) attached to an Äkta Prime Plus liquid chromatography system (GE lifesciences). The *hs*Impβ-sfGFP was then eluted with buffer B (50 mM Tris-Cl, pH 8.0, 100 mM NaCl, and 200 mM Imidazole) and further purified on a 5 mL HiTrap Q HP column (GE lifesciences), washed with 20 mM Tris-Cl, pH 7.5, 50 mM NaCl and eluted with gradient addition of 20 mM Tris-Cl, pH 7.5, 1 M NaCl. The eluted protein was concentrated using an Amicon Ultra-15 centrifugal filter (30,000 Da cutoff, MerckMillipore).

***hs*Impβ-sfGFP Q220AzF and *hs*Impβ-sfGFP Y255AzF**: *Escherichia coli* BL21(DE3) chemical competent cells were heat-shock transformed with the plasmids pDULE_CNPheRS (1) and pCDFDuet1_*hs*Impβ^{Q220TAG}-sfGFP-His_6 or pCDFDuet1_*hs*Impβ^{Y255TAG}-sfGFP-His_6 and grown overnight in 100 mL of 2YT media with Spectinomycin (25 µg/mL) and Tetracyclin (12.5 µg/mL) with shaking at 220 rpm at 37°C. Next morning, 1 L 2YT media with Spectinomycin (25 µg/mL) and Tetracyclin (12.5 µg/mL) were inoculated at OD_{600} ~0.1 and grown till OD_{600} reached 0.2 – 0.3, when the unnatural amino acid AzF (1 mM, final) was added and the protein expression was induced by adding IPTG (500 µM, final) and let grow for another 5 h. The cells were harvested by centrifugation at 4,800 rotations per minute (rpm), snap frozen in liquid Nitrogen and stored at -80°C. The purification from the cell pellets is essentially the same as described above for *hs*Impβ-sfGFP.

Protein labeling: The purified *hs*Impβ-sfGFP Q220AzF was incubated on rocker at 4°C for 2 h with 200 µL bed volume of HisPur Ni-NTA beads (Thermo Fischer). The beads were washed twice with 1×PBS, pH 7.5 and 5 µL of freshly prepared 10 mg/mL of DBCO-Fl-545 was added. The mixture was incubated for another 2 h on rocker at 4°C, covered in aluminum foil. The beads were extensively washed with 1×PBS, pH 7.5 and finally eluted with 1×PBS,

pH 7.5 supplemented with 200 mM Imidazole. The labeled protein was directly loaded onto a Native-PAGE gel and scanned on Typhoon 9400 Variable Mode Imager. The region of the scanned image showing both sfGFP and Fl-545 emission was used as background to 'cut' the corresponding region from the Native-PAGE gel. The gel pieces were transferred to a D-Tube Dialyzer Midi (MerckMillipore) tube followed by electroelution in 25 mM Tris-Cl, pH 8.0, 100 mM NaCl and 1 mM ethylenediaminetetraacetic acid, on a horizontal gel electrophoresis system. The electroeluted protein was concentrated on a Vivaspin 500 centrifugal concentrator, glycerol (5% final) added, aliquoted in 10 µL volumes, snap frozen in liquid nitrogen and stored at -80°C.

Western blotting: The protein samples (10 or 20 µL) were run on a 8% Tris-Cl-SDS polyacrylamide gel electrophoresis (PAGE) gel, followed by transfer on Immobilon-P PVDF membrane for 50 min at 50 V. The membrane was blocked with 3% Bovine serum albumin prepared in 1 ×PBS, pH 7.5, for 30 min on rocker at 4°C followed by addition of mouse monoclonal anti-His antibody (1:10,000 dilution) in the above buffer, and incubating for additional 1 h. The membrane was washed three times with 30 mL of 1 ×PBS, pH 7.5, 0.02% Tween-20 for 10 minutes each and transferred in 5% skimmed milk in 1 ×PBS, pH 7.5. The HRP-conjugated anti-Mouse IgG (1:5,000 dilution) was added and incubated for 1 h at 4°C. The membrane was washed two times with 30 mL of 1 ×PBS, pH 7.5, 0.02% Tween-20 for 10 minutes each and once with 1 ×PBS, pH 7.5, 0.05% Tween-20 for 10 minutes. The ECL Prime solution was prepared as per manufacturer's protocol and spread on the membrane, and developed on a chemiluminescence Hyperfilm.

In-gel fluorescence: The Typhoon 9400 Variable Mode Imager (GE Lifesciences) was used for all the in-gel fluorescence scans. The settings for detecting sfGFP (excitation with 488 nm

blue laser, emission filter 520 nm, band pass 40 nm) and Fl-545 (excitation with 532 nm green laser, emission filter 580 nm, band pass 30 nm) was used. Additionally, different PMT gains (200 – 400 V) were used in conjugation with 100 or 200 µm resolution. The scanned images were processed with FluorSep 2.2 and/ or ImageQuant 5.2 (Molecular Dynamics) for visualization and preparing the 'merge' image (Figures 4, S5 and S7).

Nuclear import in permeabilized cells: For import of recombinant Impβ, 80.000 HeLa P4 cells (2) were grown on poly-L-lysine-coated cover slips, washed with cold transport buffer (TB, 20 mM HEPES pH 7.3, 110 mM KOAc, 2 mM $Mg(OAc)_2$, 1 mM EGTA, 1 µg/mL aprotinin, 1 µg/mL leupeptin, 1 µg/mL pepstatin, 2 mM DTT), and permeabilized on ice with 0.007% digitonin in TB. After three washing steps with TB, cells were incubated with Impβ-GFP proteins (diluted 1:20 from stock) at room temperature for 30 min in the presence of an energy-regenerating system (1 mM ATP, 5 mM creatine phosphate, 20 U/mL creatine phosphokinase) and 1 mg/mL BSA. After import, the cells were washed with TB and nuclei were stained with 2 µg/mL Hoechst 33258 (Sigma) in PBS for 2 min. The cover slips were dried and mounted with Dako Fluorescent Mounting Medium. Images were acquired with an LSM 510 META Laser Scanning Microscope (Carl Zeiss) and processed using the LSM image browser and Fiji.

Fluorescence Lifetime Measurements: Fluorescence lifetime measurements were performed on a MicroTime 200 confocal microscope system (PicoQuant, Berlin, Germany). The system is based on an inverse epi-fluorescence microscope (IX-71, Olympus Europa) with a water immersion objective (UPLSAPO 60 x W, 1.2 N.A., Olympus Hamburg, Germany). For fluorescence excitation and lifetime measurements, we used pulsed diode lasers (LDH-P-C-470, 470 nm, PicoQuant) with linear polarization, pulse duration of 50 psec (FWHM), 40

MHz repetition rate. Fluorescence excitation and detection is done through the same objective (epi-fluorescence configuration). Collected fluorescence light is passed through a dichroic mirror (490 dcxr, Chroma Technology, Rockingham, VT, USA), and then focused by a tube lens through a 150 µm diameter confocal pinhole. After the pinhole, the light is re-collimated, split by a 50/50 beam splitter, and focused onto two single photon avalanche diodes (tau-SPAD, PicoQuant, Berlin, Germany). Emission band-pass filters (HC520/35, Semrock, USA) are positioned in front of each detector to discriminate fluorescence against scattered light. Time-correlated single-photon counting electronics (HydraHarp 400, PicoQuant GmbH) record the detected photons of all detectors independently with an absolute temporal resolution of 32 psec on a common time frame. Data for all measurements were acquired for 15 min to achieve sufficiently good photon statistics.

The routines for fluorescence lifetime calculation and analysis were implemented in MATLAB (MathWorks, Inc.). A simple biexponential model was employed for fitting only the tail (> 1 ns after laser pulse) of the fluorescence decay curve. This analysis gives all information required for calculating FRET efficiencies by means of fluorescence life time change. The tail-fitting approach avoids all the complications associated with a full deconvolution of the fluorescence decay curve with an a priori measured instrumental response function, without reducing in any way the desired information about FRET efficiencies. FRET efficiencies were calculated from the difference between the mean lifetime value of the FRET sample and that of the donor-only control in the same buffer.

MD Simulations: All bonds were constrained using the LINCS algorithm (3). An integration time step of 2 fs was used. Lennard-Jones interactions were calculated with a cut-off of 10 Å. Electrostatic interactions were calculated explicitly at a distance smaller than 10 Å; long-range electrostatic interactions were calculated by particle-mesh Ewald summation with a grid spacing of 0.12 nm and fourth order B-spline interpolation. The temperature was kept at T =

300 K, using Berendsen coupling with a coupling time of τ_T = 0.1 ps (4). Structures were recorded every 1 ps for subsequent analysis. Simulations in water and in methanol were performed in the NPT ensemble. The pressure was coupled to a Berendsen barostat with τ_p = 1.0 ps and an isotropic compressibility of 4.5×10^{-5} bar^{-1} in the x, y, and z directions (4).

All systems were energy minimized, followed by relaxation for 500 ps at 300 K, with positional restraints on the protein heavy atoms by using a force constant of k = 1000 kJ mol^{-1} nm^{-2}. All simulations were performed using periodic boundary conditions.

Radii of gyration were calculated with the GROMACS tool *g_gyrate*. The statistical uncertainty of the averaged radii of gyration was estimated as follows:

For each of the *i* trajectories, the average radius of gyration, R^i_g and its standard deviation s_i were calculated. From these values, the standard errors of the mean (σ_i) were calculated as

$$\sigma_i = \frac{s_i}{\sqrt{t/\tau_i}},$$

where t_i is the length of the simulation and τ_i the autocorrelation time of the fluctuations of the radius of gyration. From the individual values of σ_i, an average error was calculated as

$$\sigma_A = \sqrt{\frac{1}{n}\sum_{i=1}^{n}\sigma_i^2},$$

where *n* is the number of individual trajectories. σ_A describes the error due to the fluctuations of R_g within each trajectory.

As a second source of statistical uncertainty, the error corresponding to the standard deviation *s* of the R^i_g values was calculated as

$$\sigma_B = \frac{s}{\sqrt{n}}.$$

For a conservative estimate of the overall statistical uncertainty we therefore assume

$$\sigma_A = \sqrt{\frac{1}{n}\sum_{i=1}^{n}\sigma_i^2} \quad .$$

Running averages were calculated with a Gaussian kernel of 1 ns width.

Supplementary Figure 1: Importin-β in aqueous solution.

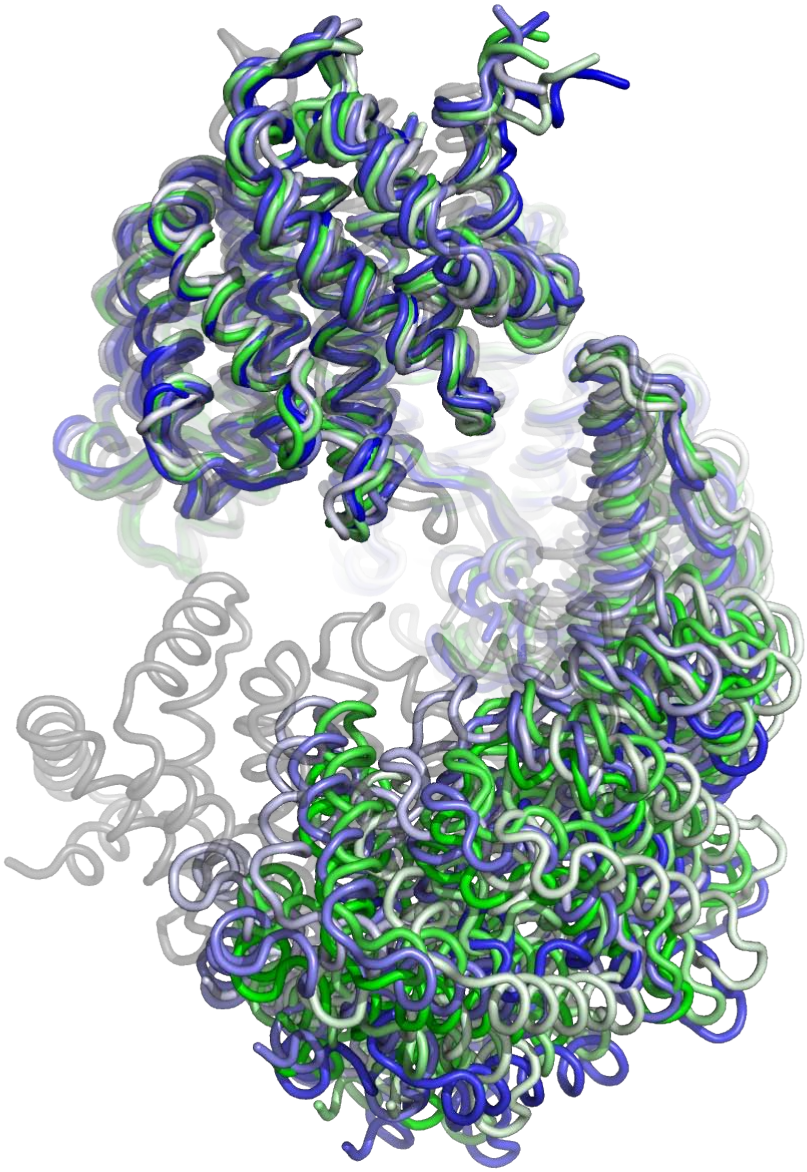

The most representative structures from a cluster analysis of Importin-β:sIBB (from the most populated cluster in green to the least populated one in blue) are aligned to the crystal structure (in grey) on the C-terminal arch.

Supplementary Figure 2: MD simulations in water.

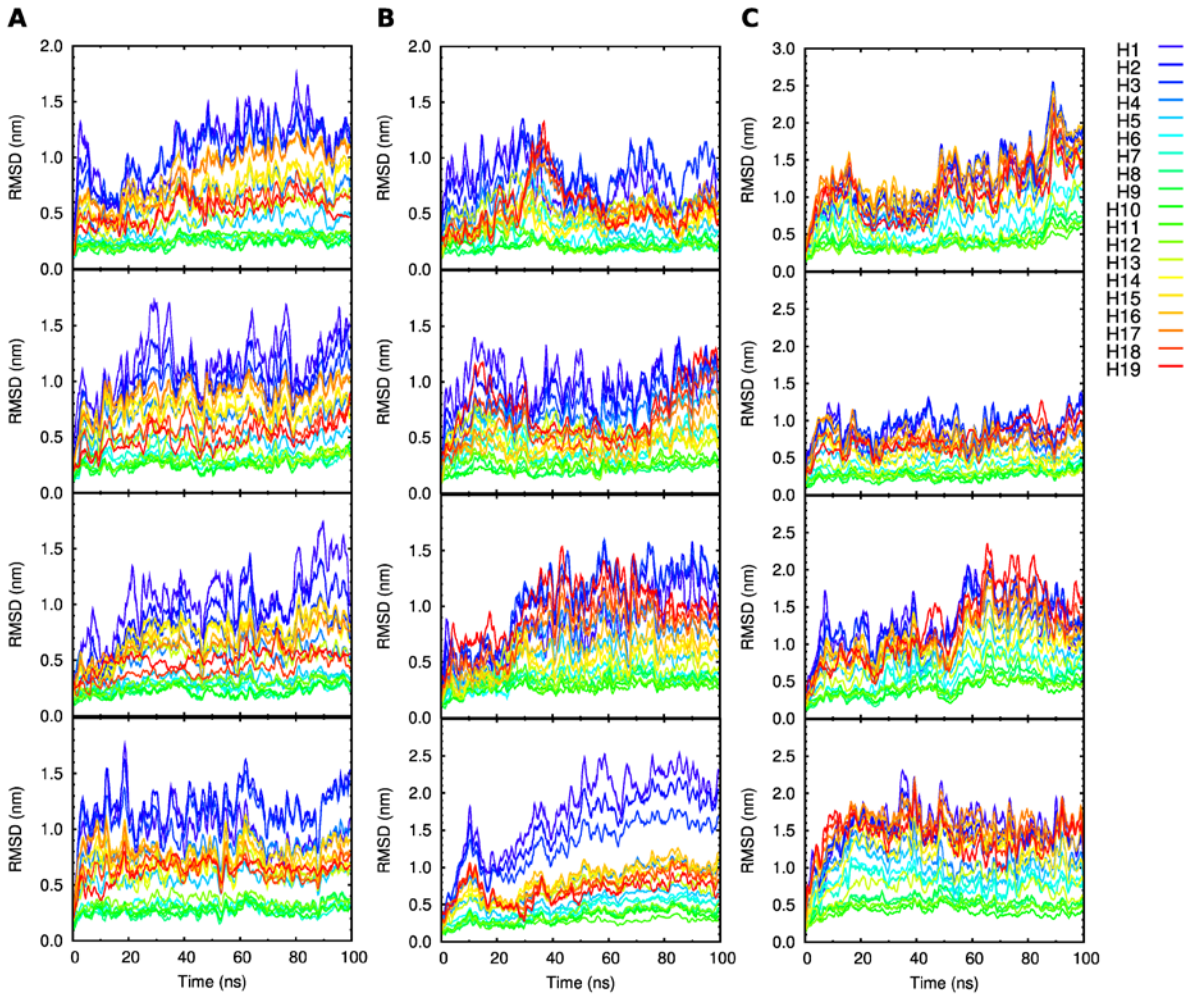

Change in root-mean-square deviation (RMSD) by HEAT repeats during simulation in water. (A) Importin-β:sIBB complex (B) Importin-β:αIBBcomplex (C) Free Importin-β (after removal of the sIBB domain). Four independent simulations each are shown. The structures were first aligned to the closed crystal structure using all backbone atoms, and, subsequently, the RMSD was calculated for each HEAT repeat separately.

Supplementary Figure 3: Simulated SAXS profile of free Importin-β in water.

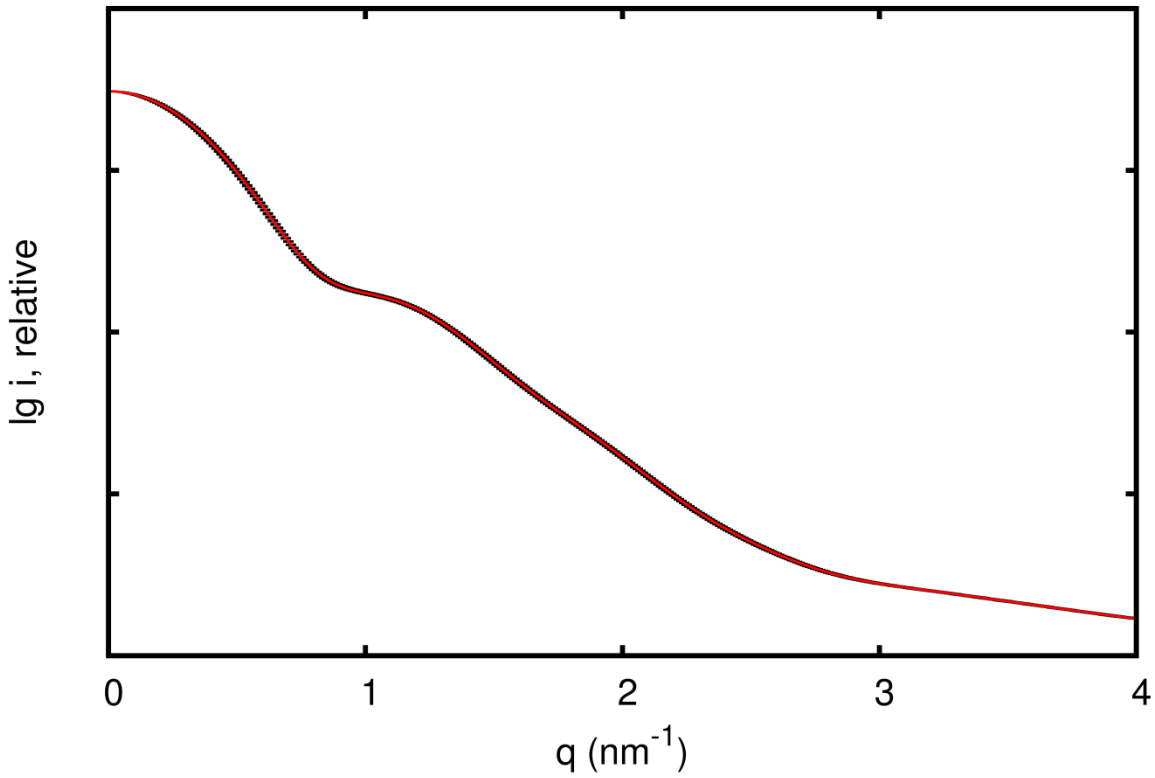

Scattering profiles were calculated on a total of 200 snapshots from the last 50 ns of the four independent trajectories and subsequently averaged. The errors were estimated by bootstrapping.

Supplementary Figure 4: MD simulations in methanol.

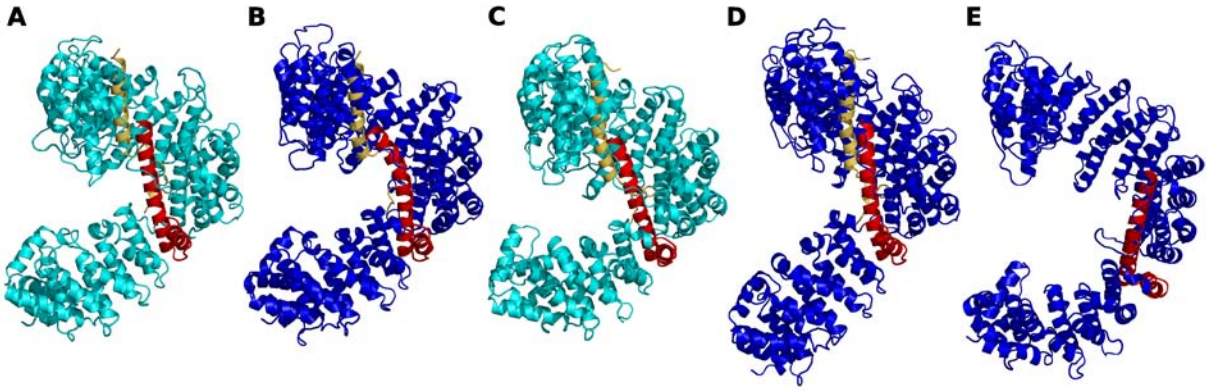

Starting conformations. (A, B) Importin-β:sIBB complex with undistorted (A) and distorted (B) HEAT repeats. (C, D) Importin-β:αIBB complex as half open (C) and completely open (D) structure. (E) Free Importin-β. H7 is shown in red, the IBB domains are shown in yellow.

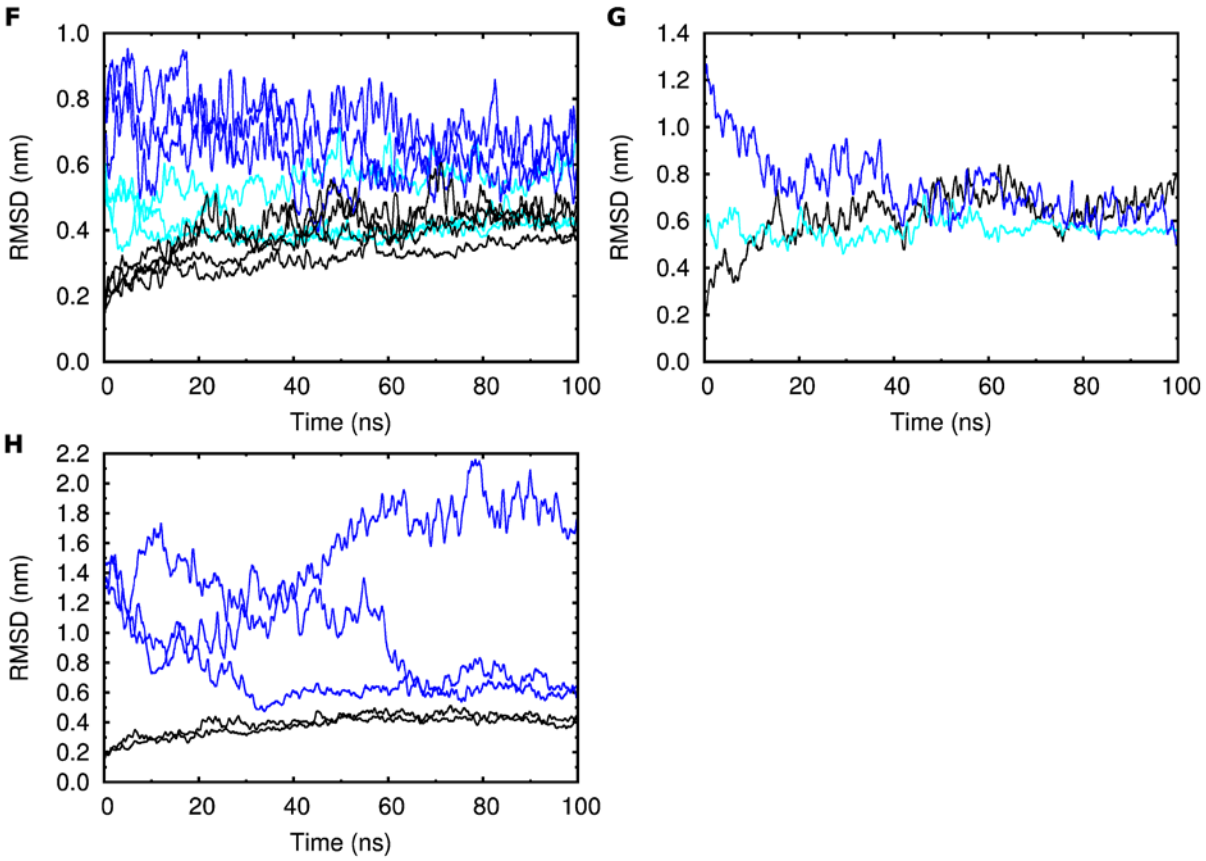

Changes in root-mean-square deviation (RMSD) during the simulations. RMSD with respect to the corresponding closed crystal structure for Importin-β:sIBB (F), Importin-β:αIBB (G), and free Importin-β (H). Simulations started from open (blue), undistorted half open (cyan) and closed (black) conformations.

Supplementary Figure 5: Spectral properties of *hs*Importin-β-sfGFP.

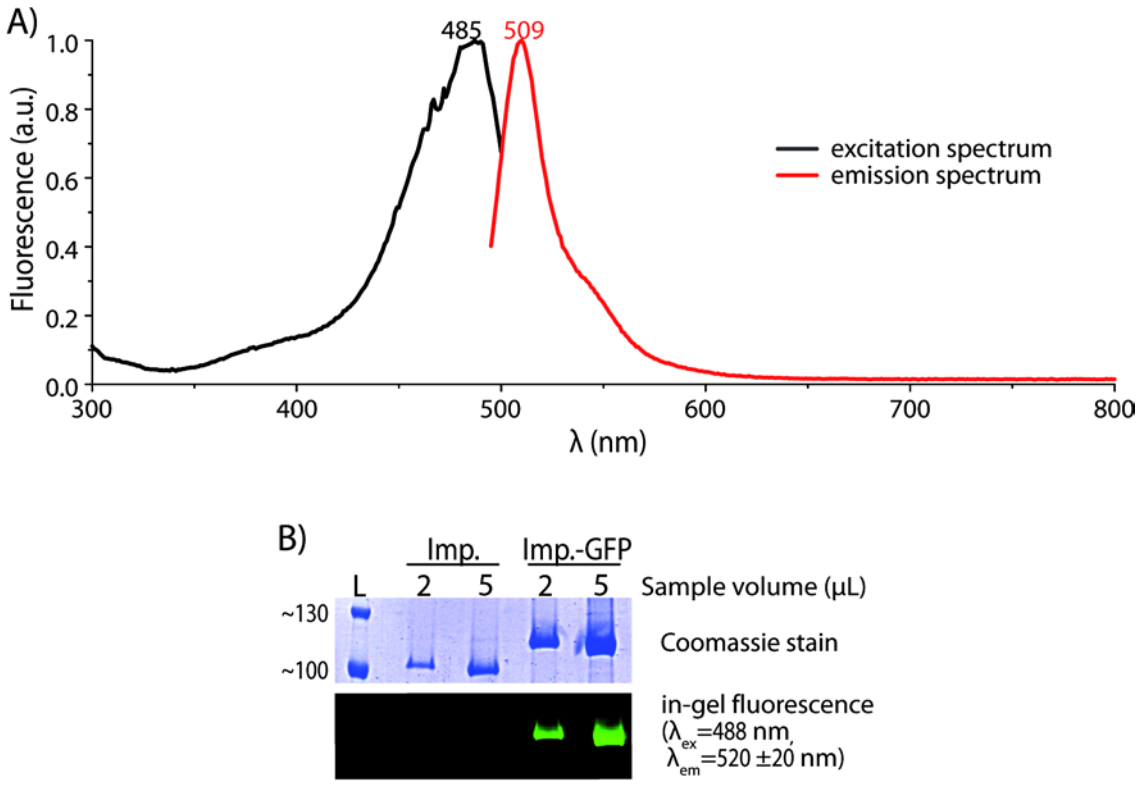

A) Excitation and emission spectra of *hs*Importin-β-GFP. B) In-gel fluorescence spectrum of *hs*Importin-β-sfGFP. L: Prestained Protein Ladder.

Supplementary Figure 6: Incorporation of AzF in hsImportin-β.

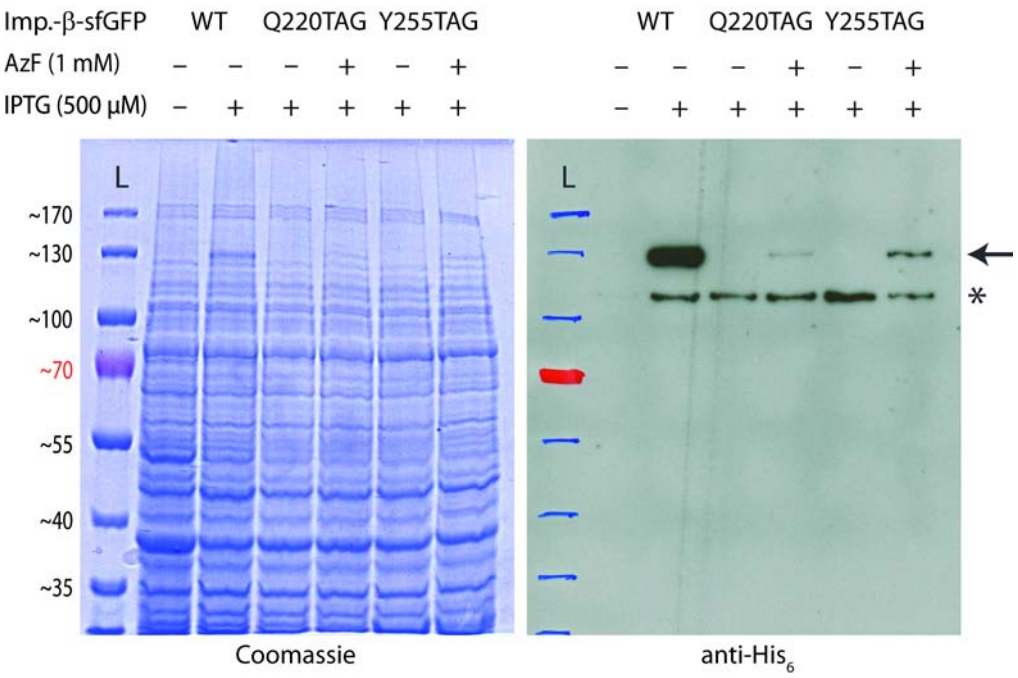

BL21 DE3 cells were transformed with plasmids encoding *hs*Importin-β with amber codons replacing codons Q220 or Y255 and pDULE CNPheRS. Cells were grown in the presence or absence of IPTG and AzF as indicated and analyzed by SDS-PAGE and Western blot. Arrow indicates the position of *hs*Importin-β, an unspecific anti-His_6 antibody cross-reactive band is indicated by an asterisk.

Supplementary Figure 7: Purification and labeling of *hs*Importin-β-sfGFP.

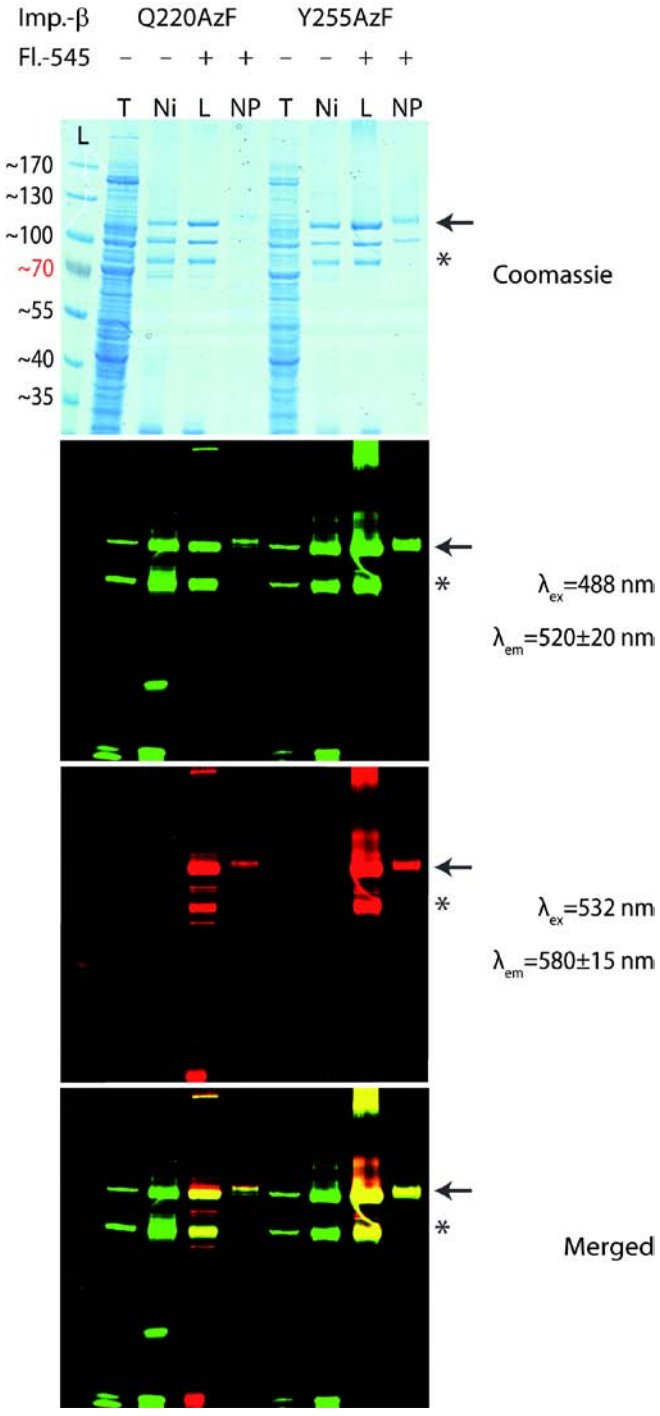

*hs*Importin-β-GFP proteins were extracted (T), purified by Ni^{2+}-affinity chromatography (Ni), labeled with Fl.-545-DBCO (L) and purified by native-PAGE (NP). Samples from all stages were analyzed by SDS-PAGE and in-gel fluorescence measured on a Typhoon phosphoimager. Arrow indicates the position of full-length *hs*Importin-β, a proteolytic fragment of *hs*Importin-β is indicated by an asterisk.

Supplementary Figure 8: Fluorescence emission spectra of *hs*Importin-β-sfGFP and *hs*Importin-β-GFP Q220AzF-Fl.-545.

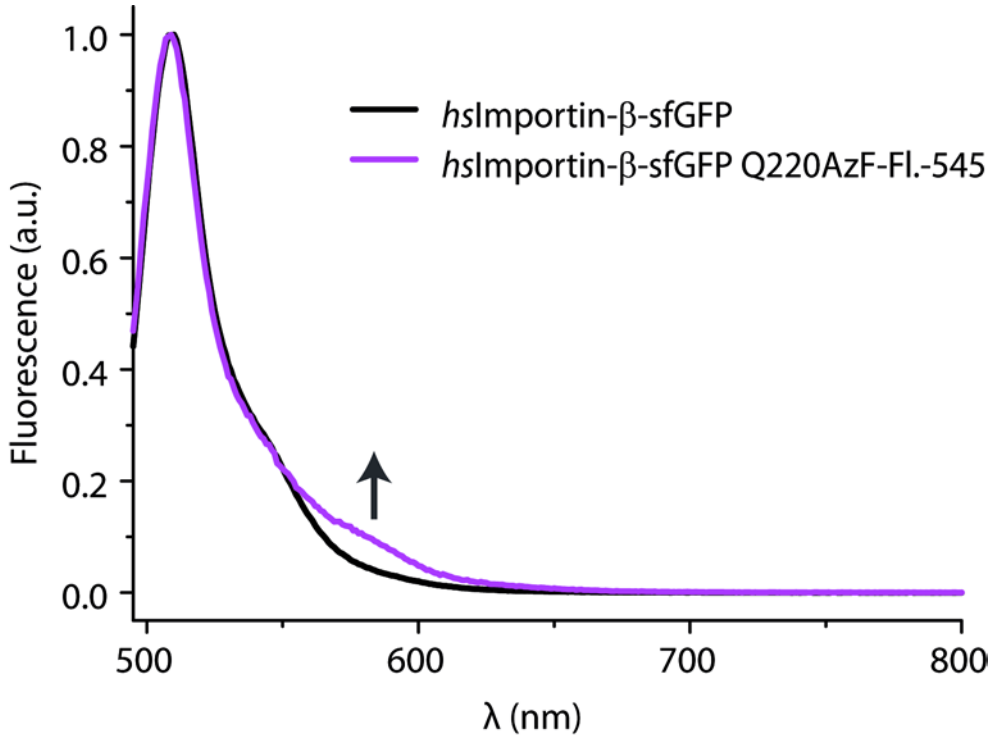

Fluorescence emission spectra of *hs*Importin-β-sfGFP and *hs*Importin-β-GFP Q220AzF-Fl.-545 were acquired using $\lambda_{ex.}$=470 nm. Coupling of the fluorophore leads to an increased emission at 575 nm.

Supplementary Figure 9: FRET in *hs*Importin-β-sfGFP Q220AzF-Fl.-545 is Proteinase K sensitive.

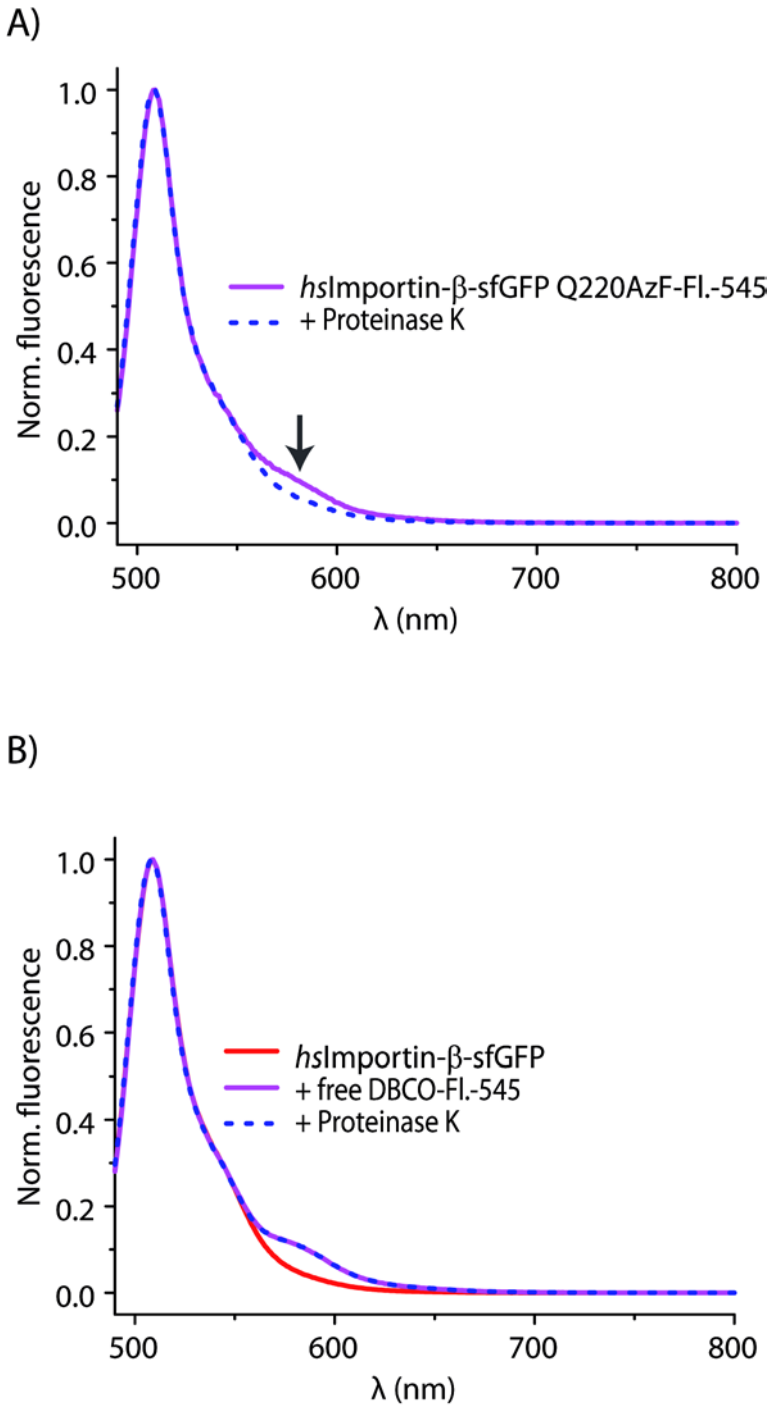

A) Fluorescence emission scans of *hs*Importin-β-sfGFP Q220AzF-Fl.-545 were taken before and after treatment with Proteinase K. B) Fluorescence emission scans of *hs*Importin-β-sfGFP were taken before and after the addition of free DBCO-Fl.-545 dye and after subsequent treatment with Proteinase K.

Supplementary Figure 10: Localization of *hs*Importin-β-sfGFP Q220AzF-Fl.-545 in permeabilized HeLa cells.

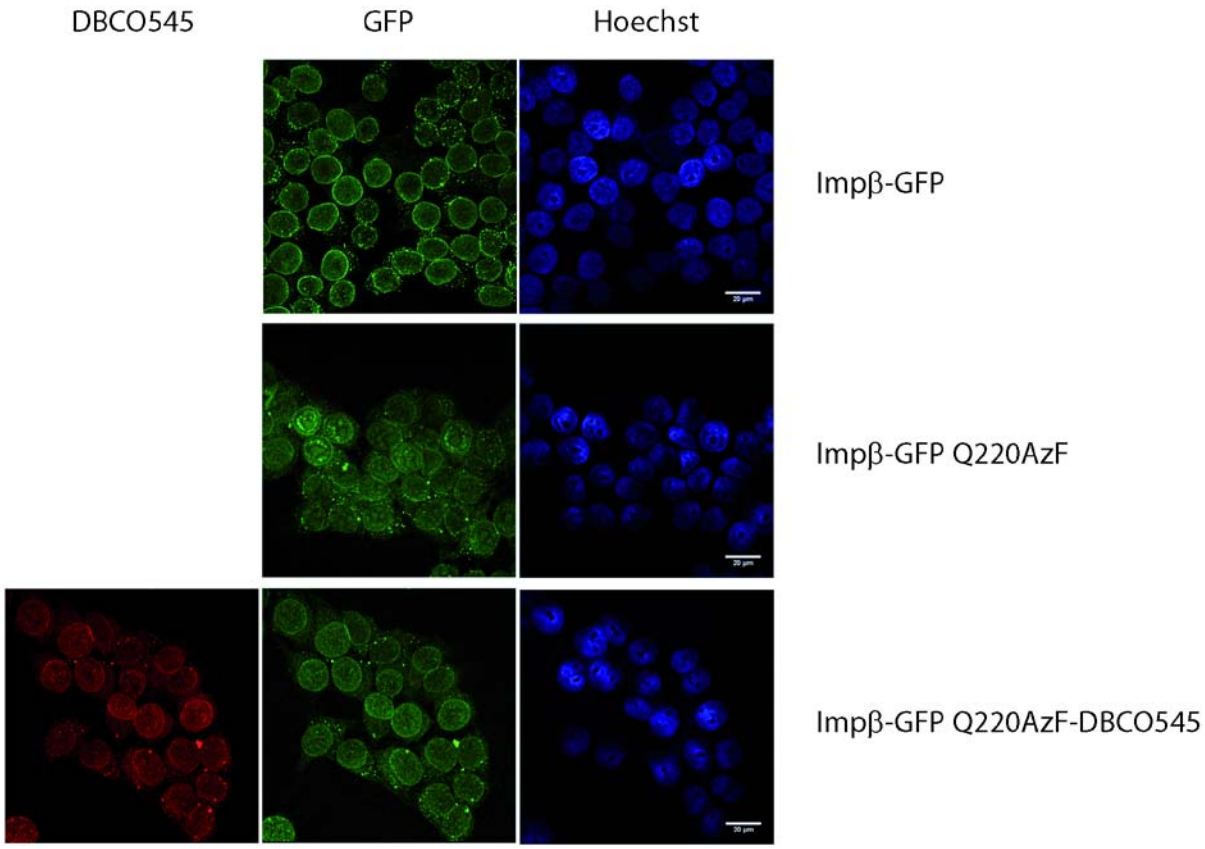

Permeabilized HeLa cells were incubated with indicated purified proteins, stained with Hoechst dye and imaged by fluorescence microscopy.

Supplementary Figure 11: Titration of methanol induces FRET in *hs*Importin-β-sfGFP Q220AzF-Fl.-545.

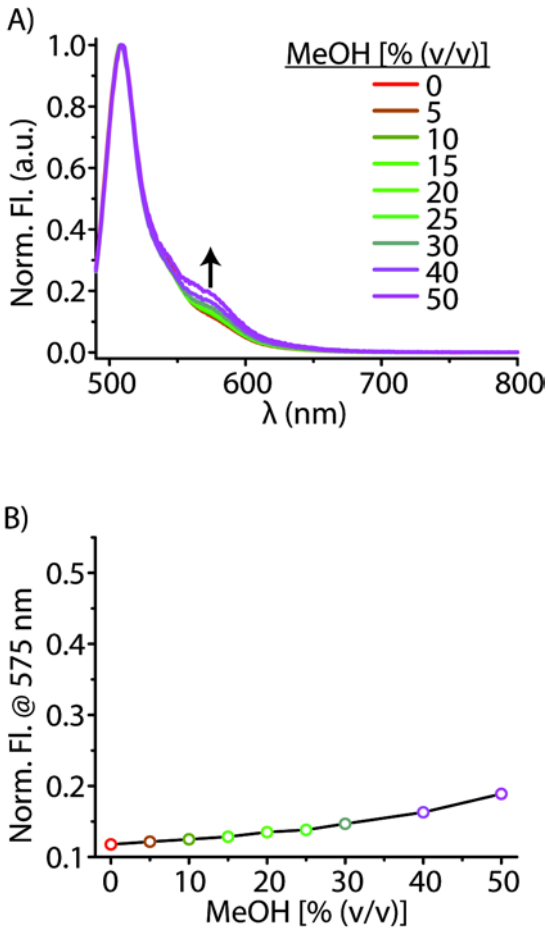

A-B) Increasing concentrations of methanol were added to *hs*Importin-β-sfGFP Q220AzF-Fl.-545. Between each addition fluorescence emission scans were acquired. Fluorescence was normalized for each spectrum setting the highest peak to 1.0.

Supplementary Figure 12: Addition of PEG induces increased FRET in *hs*Importin-β-sfGFP Q220AzF-Fl.-545.

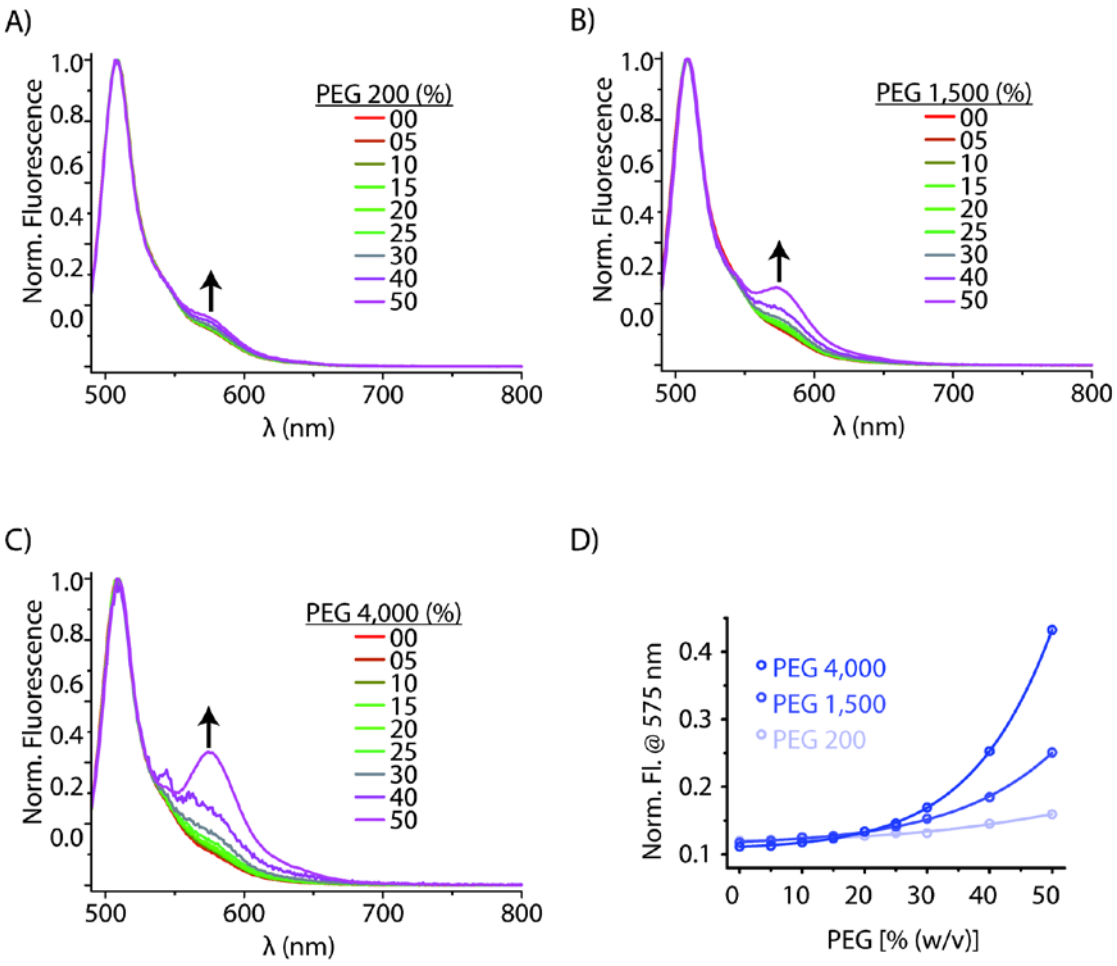

A-C) Increasing amounts of PEG of the indicated molecular weight were added to *hs*Importin-β-sfGFP Q220AzF-Fl.-545. Between each addition fluorescence emission scans were acquired. Fluorescence was normalized for each spectrum setting the highest peak to 1.0. D) Emission intensities at 575 nm of panels A-C were plotted against PEG concentration.

Supplementary Figure 13: Increasing PEG concentrations do not affect individual fluorophore properties.

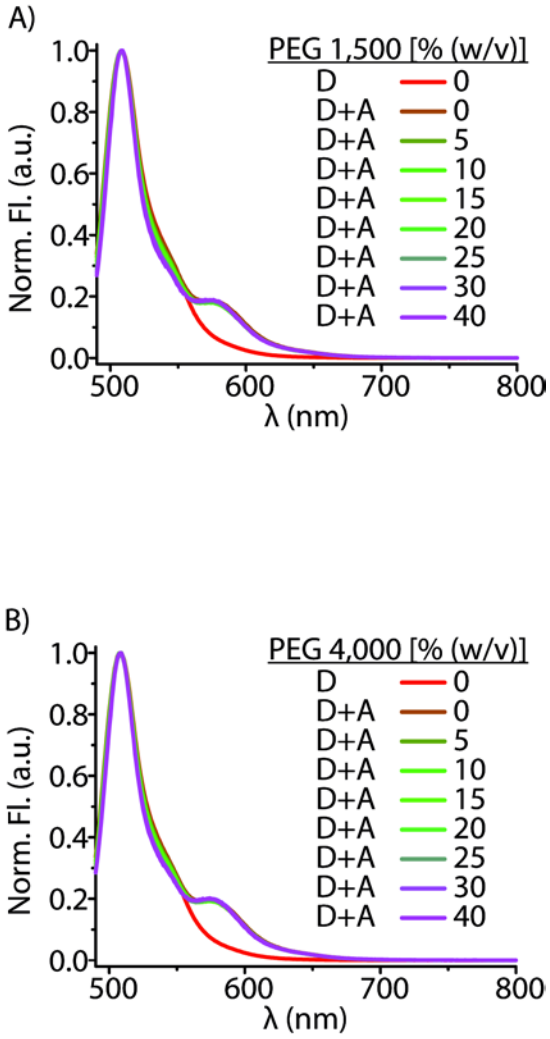

Increasing PEG concentrations do not affect the individual fluorescence properties of donor (D, *hs*Importin-β-sfGFP) and acceptor (A, DBCO-Fl.-545) dyes. A-B) *hs*Importin-β-sfGFP and DBCO-Fl.-545 were mixed in buffer and increasing concentrations of PEG of the indicated molecular weight were added stepwise. Between each addition fluorescence emission spectra were acquired ($\lambda_{ex.}$=470 nm).

Supplementary Figure 14: Titration of Ficoll-70 does not induce significantly increased FRET in *hs*Importin-β-sfGFP Q220AzF-Fl.-545.

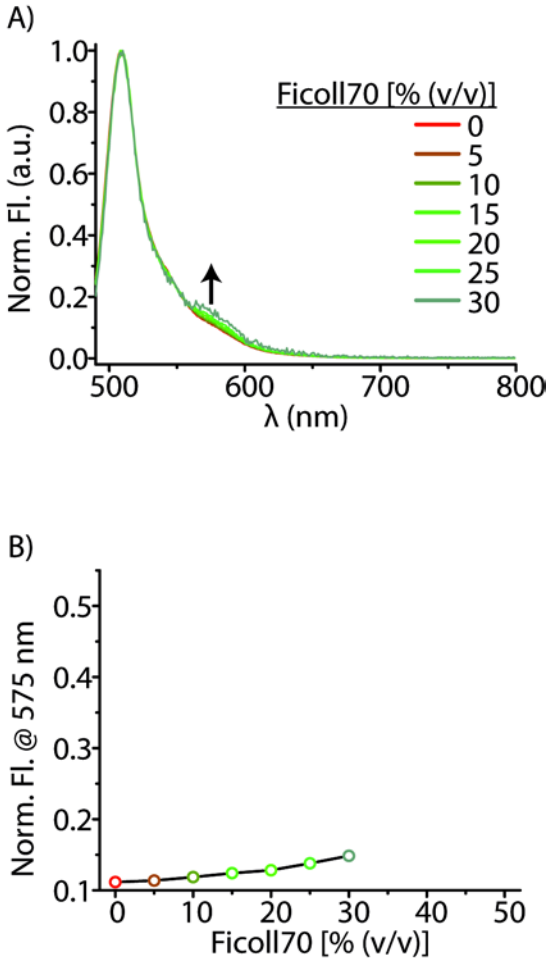

A) Increasing amounts of Ficoll-70 was added to *hs*Importin-β-sfGFP Q220AzF-Fl.-545. Between each addition fluorescence emission scans were acquired. Fluorescence was normalized for each spectrum setting the highest peak to 1.0. B) Emission intensities at 575 nm of panel A was plotted against Ficoll-70 concentration. For technical reasons a concentration above 30% could not be reached.

Supplementary Figure 15: Reversibility of PEG induced FRET increase in *hs*Importin-β-sfGFP Q220AzF-Fl.-545.

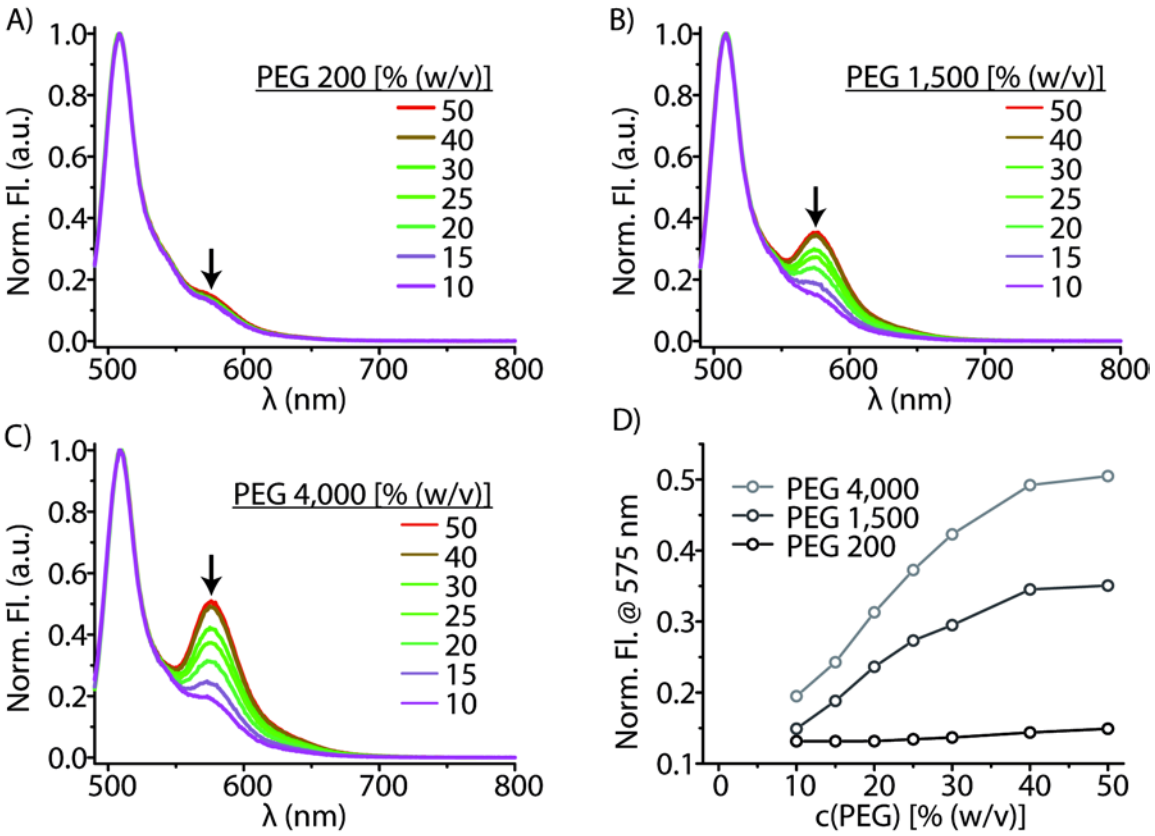

A-C) Starting from a *hs*Importin-β-sfGFP Q220AzF-Fl.-545 solution containing a concentration of 50% PEG of the indicated molecular weight buffer is added stepwise. Between each addition fluorescence emission scans were acquired. Fluorescence was normalized for each spectrum setting the highest peak to 1.0. D) Emission intensities at 575 nm of panels A-C were plotted against PEG concentration.

Supplementary Figure 16: Donor fluorescence lifetime measurements.

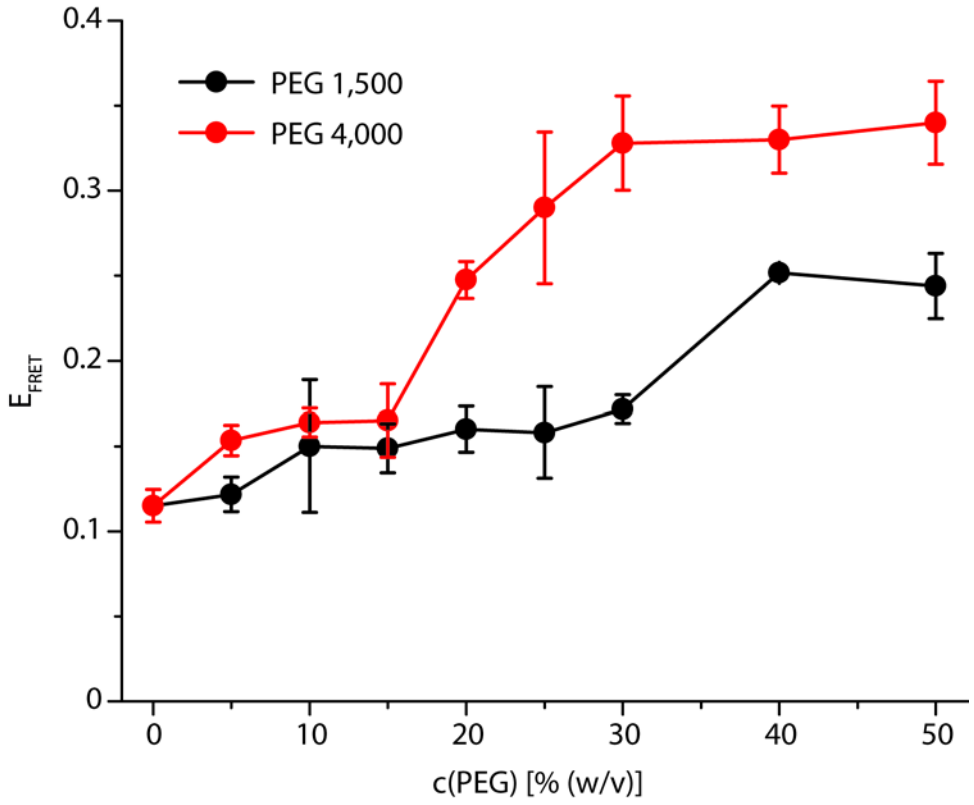

Addition of PEG 1,500 or PEG 4,000 increases relative FRET efficiency in *hs*Impβ-sfGFP Q220AzF-Fl.-545 determined by donor fluorescence lifetime measurements. Error bars represent standard error of the mean.

Supplementary Table S1

Importin-β in complex with	Simulations in water	Simulations in methanol
sIBB	4 x 100 ns (PDBid 2P8Q)	4 x 100 ns (PDBid 2P8Q) 3 x 100 ns (snapshot from simulations in water, Rg=3.4 nm, undistorted) 3 x 100 ns (snapshot from simulations in water, Rg=3.5 nm, distorted)
αIBB	4 x 100 ns (PDBid 2QGK)	1 x 100 ns (PDBid 2QGK) 1 x 100 ns (snapshot from simulations in water, Rg=3.4 nm) 1 x 100 ns (snapshot from simulations in water, Rg=3.7 nm)
---	3 x 100 ns (PDBid 2P8Q, after removal of sIBB) 1 x 100 ns (PDBid 2QGK, after removal of αIBB)	2 x 100 ns (PDBid 2P8Q, after removal of sIBB) 3 x 100 ns (snapshot from simulations in water, Rg=3.9 nm)

Table S1: Summary of simulations with their corresponding initial conformations (in parentheses).

Supplementary Table S2

PDBid	Importin-β in complex with	Crystallization condition Mother liquor	Cryo condition in addition to mother liquor	Confor-mation
1QGK (5)	αIBB	18-22% PEG 8000, 50 mM potassium acetate (pH 5.8), 10 mM β-mercaptoethanol	prolonged dehydration (1-7 days) 25% PEG 400	closed
1QGR (5)	αIBB	16-20% PEG 8000, 50 mM potassium phosphate (pH 3.9), 10 mM β-mercaptoethanol, 5 mM NaI	prolonged dehydration 25% PEG 400	closed

1UKL (6)	SREBP-2	5-6% PEG 8000, 10% glycerol, 50 mM MES buffer (pH 6.6), 30 mM $SrCl_2$	25% glycerol	open
2BKU (7)	RanGTP	14-16% PEG 3350, 100 mM MES buffer (pH 6.2), 1-2 mM MnCl	25% (w/v) glycerol	open
2BPT (8)	Nup1p	13% (w/v) PEG 8000, 5 mM Tris (pH 7.4), 50 mM sodium cacodylate (pH 6.5), 90 mM $(NH_4)_2SO_4$	10% (w/v) glycerol	closed
2P8Q (9)	sIBB	20% PEG 8000, 50 mM NaCl (pH 6.0)	prolonged dehydration 38% PEG 8000	closed
2Q5D (9)	sIBB	20% PEG 8000, 50 mM NaCl (pH 6.0)	prolonged dehydration 38% PEG 8000	closed/ open
3ND2 (10)		20% PEG 4000, 12% MPD, 0.1 M MES (pH 6.5), 20 mM $MgCl_2$, 125 mM NaCl		closed
2QNA (11)	sIBB	0.92 M $(NH_4)_2SO_4$, 2.5% ethanol	quick soak (seconds) 20% glycerol to mother liquor	open

Table S2: Comparison of crystallization conditions and Importin-β conformation.

Plasmid Sequence of pCDFDuet1_*hs*Impβ-sfGFP-His$_6$, pCDFDuet1_*hs*Impβ^{Q220TAG}-sfGFP-His$_6$ and pCDFDuet1_*hs*Impβ^{Y255TAG}-sfGFP-His$_6$: The ORF (nucleotide 71 – 3,451) is shown in lowercase and the TAG mutation sites for amino acid Q220 and Y255 is highlighted in yellow and green, respectively:

```
   1 GGGGAATTGTGAGCGGATAACAATTCCCCTGTAGAAATAATTTTGTTTAACTTTAATAAG 60
  61 GAGATATAccatggagctgatcaccattctcgagaagaccgtgtctcccgatcggctgga 120
 121 gctggaagcggcgcagaagttcctggagcgtgcggccgtggagaacctgcccactttcct 180
 181 tgtggaactgtccagagtgctggcaaatccaggaaacagtcaggttgccagagttgcagc 240
 241 tggtctacaaatcaagaactctttgacatctaaagatccagatatcaaggcacaatatca 300
 301 gcagaggtggcttgctattgatgctaatgctcgacgagaagtcaagaactatgttttgca 360
 361 gacattgggtacagaaacttaccggcctagttctgcctcacagtgtgtggctggtattgc 420
 421 ttgtgcagagatcccagtaaaccagtggccagaactcattcctcagctggtggccaatgt 480
 481 cacaaaccccaacagcacagagcacatgaaggagtcgacattggaagccatcggttatat 540
 541 ttgccaagatatagacccagagcagctacaagataaatccaatgagattctgactgccat 600
 601 aatccaggggatgaggaaagaagagcctagtaataatgtgaagctagctgctacgaatgc 660
 661 actcctgaactcattggagttcaccaaagcaaactttgataaagagtctgaaaggcactt 720
 721 tattatgcaggtggtctgtgaagccacacagtgtccagatacgagggtacgagtggctgc 780
 781 tttacagaatctggtgaagataatgtccttatattatcagtacatggagacatatatggg 840
 841 tcctgctctttttgcaatcacaatcgaagcaatgaaaagtgacattgatgaggtggcttt 900
 901 acaagggatagaattctggtccaatgtctgtgatgaggaaatggatttggccattgaagc 960
 961 ttcagaggcagcagaacaaggacggccccctgagcacaccagcaagttttatgcgaaggg 1020
1021 agcactacagtatctggttccaatcctcacacagacactaactaaacaggacgaaaatga 1080
1081 tgatgacgatgactggaacccctgcaaagcagcaggggtgtgcctcatgcttctggccac 1140
1141 ctgctgtgaagatgacattgtcccacatgtcctccccttcattaaagaacacatcaagaa 1200
1201 cccagattggcggtaccgggatgcagcagtgatggcttttggttgtatcttggaaggacc 1260
1261 agagcccagtcagctcaaaccactagttatacaggctatgcccaccctaatagaattaat 1320
1321 gaaagaccccagtgtagttgttcgagatacagctgcatggactgtaggcagaatttgtga 1380
1381 gctgcttcctgaagctgccatcaatgatgtctacttggctcccctgctacagtgtctgat 1440
1441 tgagggtctcagtgctgaacccagagtggcttcaaatgtgtgctgggctttctccagtct 1500
1501 ggctgaagctgcttatgaagctgcagacgttgctgatgatcaggaagaaccagctactta 1560
1561 ctgcttatcttcttcatttgaactcatagttcagaagctcctagagactacagacagacc 1620
1621 tgatggacaccagaacaacctgaggagttctgcatatgaatctctgatggaaattgtgaa 1680
1681 aaacagtgccaaggattgttatcctgctgtccagaaaacgactttggtcatcatggaacg 1740
1741 actgcaacaggttcttcagatggagtcacatatccagagcacatccgatagaatccagtt 1800
1801 caatgaccttcagtctttactctgtgcaactcttcagaatgttcttcggaaagtgcaaca 1860
1861 tcaagatgctttgcagatctctgatgtggttatggcctccctgttaaggatgttccaaag 1920
1921 cacagctgggtctgggggagtacaagaggatgccctgatggcagttagcacactggtgga 1980
1981 agtgttgggtggtgaattcctcaagtacatggaggcctttaaacccttcctgggcattgg 2040
2041 attaaaaaattatgctgaataccaggtttgtttggcagctgtgggcttagtgggagactt 2100
2101 gtgccgtgccctgcaatccaacatcatacctttctgtgacgaggtgatgcagctgcttct 2160
2161 ggaaaatttggggaatgagaacgtccacaggtctgtgaagccgcagattctgtcagtgtt 2220
2221 tggtgatattgcccttgctattggaggagagtttaaaaaatacttagaggttgtattgaa 2280
2281 tactcttcagcaggcctcccaagcccaggtggacaagtcagactatgacatggtggatta 2340
2341 tctgaatgagctaagggaaagctgcttggaagcctatactggaatcgtccagggattaaa 2400
2401 gggggatcaggagaacgtacacccggatgtgatgctggtacaacccagagtagaatttat 2460
2461 tctgtctttcattgaccacattgctggagatgaggatcacacagatggagtagtagcttg 2520
2521 tgctgctggactaataggggacttatgtacagcatttgggaaggatgtactgaaattagt 2580
2581 agaagctaggccaatgatccatgaattgttaactgaagggcggagatcgaagactaacaa 2640
2641 agcaaaaacccttgctacatgggcaacaaaagaactgaggaaactgaagaaccaagctgg 2700
2701 atctCAATTGgttagcaaaggtgaagaactgtttaccggcgttgtgccgattctggtgga 2760
2761 actggatggtgatgtgaatggccataaatttagcgttcgtggcgaaggcgaaggtgatgc 2820
2821 gaccaacggtaaactgaccctgaaatttatttgcaccaccggtaaactgccggttccgtg 2880
2881 gccgaccctggtgaccaccctgacctatggcgttcagtgctttagccgctatccggatca 2940
2941 tatgaaacgccatgatttctttaaaagcgcgatgccggaaggctatgtgcaggaacgtac 3000
3001 cattagcttcaaagatgatggcacctataaaacccgtgcggaagttaaatttgaaggcga 3060
```

3061 taccctggtgaaccgcattgaactgaaaggtattgattttaaagaagatggcaacattct 3120
3121 gggtcataaactggaatataatttcaacagccataatgtgtatattaccgccgataaaca 3180
3181 gaaaaatggcatcaaagcgaactttaaaatccgtcacaacgtggaagatggtagcgtgca 3240
3241 gctggcggatcattatcagcagaataccccgattggtgatggcccggtgctgctgccgga 3300
3301 taatcattatctgagcacccagagcgttctgagcaaagatccgaatgaaaaacgtgatca 3360
3361 tatggtgctgctggaatttgttaccgccgcgggcattacccacggtatggatgaactgta 3420
3421 taaaggcagccaccatcatcatcaccattaaGACGTCGGTACCCTCGAGTCTGGTAAAGA 3480
3481 AACCGCTGCTGCGAAATTTGAACGCCAGCACATGGACTCGTCTACTAGCGCAGCTTAATT 3540
3541 AACCTAGGCTGCTGCCACCGCTGAGCAATAACTAGCATAACCCCTTGGGGCCTCTAAACG 3600
3601 GGTCTTGAGGGGTTTTTTGCTGAAACCTCAGGCATTTGAGAAGCACACGGTCACACTGCT 3660
3661 TCCGGTAGTCAATAAACCGGTAAACCAGCAATAGACATAAGCGGCTATTTAACGACCCTG 3720
3721 CCCTGAACCGACGACCGGGTCATCGTGGCCGGATCTTGCGGCCCCTCGGCTTGAACGAAT 3780
3781 TGTTAGACATTATTTGCCGACTACCTTGGTGATCTCGCCTTTCACGTAGTGGACAAATTC 3840
3841 TTCCAACTGATCTGCGCGCGAGGCCAAGCGATCTTCTTCTTGTCCAAGATAAGCCTGTCT 3900
3901 AGCTTCAAGTATGACGGGCTGATACTGGGCCGGCAGGCGCTCCATTGCCCAGTCGGCAGC 3960
3961 GACATCCTTCGGCGCGATTTTGCCGGTTACTGCGCTGTACCAAATGCGGGACAACGTAAG 4020
4021 CACTACATTTCGCTCATCGCCAGCCCAGTCGGGCGGCGAGTTCCATAGCGTTAAGGTTTC 4080
4081 ATTTAGCGCCTCAAATAGATCCTGTTCAGGAACCGGATCAAAGAGTTCCTCCGCCGCTGG 4140
4141 ACCTACCAAGGCAACGCTATGTTCTCTTGCTTTTGTCAGCAAGATAGCCAGATCAATGTC 4200
4201 GATCGTGGCTGGCTCGAAGATACCTGCAAGAATGTCATTGCGCTGCCATTCTCCAAATTG 4260
4261 CAGTTCGCGCTTAGCTGGATAACGCCACGGAATGATGTCGTCGTGCACAACAATGGTGAC 4320
4321 TTCTACAGCGCGGAGAATCTCGCTCTCTCCAGGGGAAGCCGAAGTTTCCAAAAGGTCGTT 4380
4381 GATCAAAGCTCGCCGCGTTGTTTCATCAAGCCTTACGGTCACCGTAACCAGCAAATCAAT 4440
4441 ATCACTGTGTGGCTTCAGGCCGCCATCCACTGCGGAGCCGTACAAATGTACGGCCAGCAA 4500
4501 CGTCGGTTCGAGATGGCGCTCGATGACGCCAACTACCTCTGATAGTTGAGTCGATACTTC 4560
4561 GGCGATCACCGCTTCCCTCATACTCTTCCTTTTTCAATATTATTGAAGCATTTATCAGGG 4620
4621 TTATTGTCTCATGAGCGGATACATATTTGAATGTATTTAGAAAAATAAACAAATAGCTAG 4680
4681 CTCACTCGGTCGCTACGCTCCGGGCGTGAGACTGCGGCGGGCGCTGCGGACACATACAAA 4740
4741 GTTACCCACAGATTCCGTGGATAAGCAGGGGACTAACATGTGAGGCAAAACAGCAGGGCC 4800
4801 GCGCCGGTGGCGTTTTTCCATAGGCTCCGCCCTCCTGCCAGAGTTCACATAAACAGACGC 4860
4861 TTTTCCGGTGCATCTGTGGGAGCCGTGAGGCTCAACCATGAATCTGACAGTACGGGCGAA 4920
4921 ACCCGACAGGACTTAAAGATCCCCACCGTTTCCGGCGGGTCGCTCCCTCTTGCGCTCTCC 4980
4981 TGTTCCGACCCTGCCGTTTACCGGATACCTGTTCCGCCTTTCTCCCTTACGGGAAGTGTG 5040
5041 GCGCTTTCTCATAGCTCACACACTGGTATCTCGGCTCGGTGTAGGTCGTTCGCTCCAAGC 5100
5101 TGGGCTGTAAGCAAGAACTCCCCGTTCAGCCCGACTGCTGCGCCTTATCCGGTAACTGTT 5160
5161 CACTTGAGTCCAACCCGGAAAAGCACGGTAAAACGCCACTGGCAGCAGCCATTGGTAACT 5220
5221 GGGAGTTCGCAGAGGATTTGTTTAGCTAAACACGCGGTTGCTCTTGAAGTGTGCGCCAAA 5280
5281 GTCCGGCTACACTGGAAGGACAGATTTGGTTGCTGTGCTCTGCGAAAGCCAGTTACCACG 5340
5341 GTTAAGCAGTTCCCCAACTGACTTAACCTTCGATCAAACCACCTCCCCAGGTGGTTTTTT 5400
5401 CGTTTACAGGGCAAAAGATTACGCGCAGAAAAAAAGGATCTCAAGAAGATCCTTTGATCT 5460
5461 TTTCTACTGAACCGCTCTAGATTTCAGTGCAATTTATCTCTTCAAATGTAGCACCTGAAG 5520
5521 TCAGCCCCATACGATATAAGTTGTAATTCTCATGTTAGTCATGCCCCGCGCCCACCGGAA 5580
5581 GGAGCTGACTGGGTTGAAGGCTCTCAAGGGCATCGGTCGAGATCCCGGTGCCTAATGAGT 5640
5641 GAGCTAACTTACATTAATTGCGTTGCGCTCACTGCCCGCTTTCCAGTCGGGAAACCTGTC 5700
5701 GTGCCAGCTGCATTAATGAATCGGCCAACGCGCGGGGAGAGGCGGTTTGCGTATTGGGCG 5760
5761 CCAGGGTGGTTTTTCTTTTCACCAGTGAGACGGGCAACAGCTGATTGCCCTTCACCGCCT 5820
5821 GGCCCTGAGAGAGTTGCAGCAAGCGGTCCACGCTGGTTTGCCCCAGCAGGCGAAAATCCT 5880
5881 GTTTGATGGTGGTTAACGGCGGGATATAACATGAGCTGTCTTCGGTATCGTCGTATCCCA 5940
5941 CTACCGAGATGTCCGCACCAACGCGCAGCCCGGACTCGGTAATGGCGCGCATTGCGCCCA 6000
6001 GCGCCATCTGATCGTTGGCAACCAGCATCGCAGTGGGAACGATGCCCTCATTCAGCATTT 6060
6061 GCATGGTTTGTTGAAAACCGGACATGGCACTCCAGTCGCCTTCCCGTTCCGCTATCGGCT 6120
6121 GAATTTGATTGCGAGTGAGATATTTATGCCAGCCAGCCAGACGCAGACGCGCCGAGACAG 6180
6181 AACTTAATGGGCCCGCTAACAGCGCGATTTGCTGGTGACCCAATGCGACCAGATGCTCCA 6240
6241 CGCCCAGTCGCGTACCGTCTTCATGGGAGAAAATAATACTGTTGATGGGTGTCTGGTCAG 6300
6301 AGACATCAAGAAATAACGCCGGAACATTAGTGCAGGCAGCTTCCACAGCAATGGCATCCT 6360
6361 GGTCATCCAGCGGATAGTTAATGATCAGCCCACTGACGCGTTGCGCGAGAAGATTGTGCA 6420
6421 CCGCCGCTTTACAGGCTTCGACGCCGCTTCGTTCTACCATCGACACCACCACGCTGGCAC 6480
6481 CCAGTTGATCGGCGCGAGATTTAATCGCCGCGACAATTTGCGACGGCGCGTGCAGGGCCA 6540
6541 GACTGGAGGTGGCAACGCCAATCAGCAACGACTGTTTGCCCGCCAGTTGTTGTGCCACGC 6600
6601 GGTTGGGAATGTAATTCAGCTCCGCCATCGCCGCTTCCACTTTTTCCCGCGTTTTCGCAG 6660
6661 AAACGTGGCTGGCCTGGTTCACCACGCGGGAAACGGTCTGATAAGAGACACCGGCATACT 6720
6721 CTGCGACATCGTATAACGTTACTGGTTTCACATTCACCACCCTGAATTGACTCTCTTCCG 6780

```
6781 GGCGCTATCATGCCATACCGCGAAAGGTTTTGCGCCATTCGATGGTGTCCGGGATCTCGA 6840
6841 CGCTCTCCCTTATGCGACTCCTGCATTAGGAAATTAATACGACTCACTATA 6891
```

Supporting References

1. Young DD, *et al.* (2011) An evolved aminoacyl-tRNA synthetase with atypical polysubstrate specificity. *Biochemistry* **50**(11):1894-1900.
2. Charneau P, *et al.* (1994) HIV-1 reverse transcription. A termination step at the center of the genome. *J Mol Biol* **241**(5):651-662.
3. Hess B, Bekker H, Berendsen HJC, & Fraaije JGEM (1997) LINCS: A linear constraint solver for molecular simulations. *Journal of computational chemistry* **18**(12):1463-1472.
4. Berendsen HJC, Postma JPM, Vangunsteren WF, Dinola A, & Haak JR (1984) Molecular-Dynamics with Coupling to an External Bath. *J Chem Phys* **81**(8):3684-3690.
5. Cingolani G, Petosa C, Weis K, & Müller CW (1999) Structure of importin-beta bound to the IBB domain of importin-alpha. *Nature* **399**(6733):221-229.
6. Lee SJ, *et al.* (2003) The structure of importin-beta bound to SREBP-2: nuclear import of a transcription factor. *Science (New York, NY)* **302**(5650):1571-1575.
7. Lee SJ, Matsuura Y, Liu SM, & Stewart M (2005) Structural basis for nuclear import complex dissociation by RanGTP. *Nature* **435**(7042):693-696.
8. Liu SM & Stewart M (2005) Structural basis for the high-affinity binding of nucleoporin Nup1p to the Saccharomyces cerevisiae importin-beta homologue, Kap95p. *Journal of molecular biology* **349**(3):515-525.
9. Mitrousis G, Olia AS, Walker-Kopp N, & Cingolani G (2008) Molecular basis for the recognition of snurportin 1 by importin beta. *The Journal of biological chemistry* **283**(12):7877-7884.
10. Forwood JK, *et al.* (2010) Quantitative structural analysis of importin-beta flexibility: paradigm for solenoid protein structures. *Structure (London, England : 1993)* **18**(9):1171-1183.
11. Wohlwend D, Strasser A, Dickmanns A, & Ficner R (2007) Structural basis for RanGTP independent entry of spliceosomal U snRNPs into the nucleus. *Journal of molecular biology* **374**(4):1129-1138.